PHYSICAL REVIEW A VOLUME 39, NUMBER 2 JANUARY 15, 1989

# Electron-impact excitation of $Al^{2+}$

J. Mitroy* and D. W. Norcross†

*Joint Institute for Laboratory Astrophysics, University of Colorado and National Bureau of Standards,*
*Boulder, Colorado 80309-0440*

(Received 29 June 1988)

Detailed calculations of the electron-impact excitation of the sodiumlike ion $Al^{2+}$ were performed using both the unitarized Coulomb-Born approximation and the close-coupling approach. Calculations were undertaken at both the five-state (3*s*, 3*p*, 3*d*, 4*s*, and 4*p*) and nine-state ($+\overline{4d}$, $\overline{4f}$, $\overline{5s}$, and $\overline{5p}$) levels of approximation. Calculations using Hamiltonians both with and without (semiempirical) core-polarization potentials were completed. Particular attention was paid to the resonance (3*s*-3*p*) excitation. The inclusion of core-polarization potentials resulted in cross sections for the resonance excitation that are 10% smaller in magnitude. As an additional check on the calculations, binding energies of $Al^{+}$ bound states, and oscillator strengths for $Al^{2+}$ transitions, were also computed and compared with the results of measurements and other calculations.

## I. INTRODUCTION

In this paper we present the results of a detailed study of electron-impact excitation of $Al^{2+}$, with particular emphasis on the resonance (3*s*-3*p*) transition. The calculation of electron-ion cross sections is motivated primarily by the importance of cross-section information in a number of important applications, e.g., the modeling of fusion and astrophysical plasmas. While the applications aspect provides justification in itself for a calculation on $Al^{2+}$, the simplicity of the alkali-metal-like ions makes them an ideal system for detailed calculations that can perhaps provide guidance for calculations on more complicated system.

Most reported calculations of cross sections for $Al^{2+}$ to date are based on rather simple approximations: the classical binary encounter approach,[1] first Born approximation,[2] Gaunt factor approximation,[3] and distorted-wave[4] approximation. There has also been a five-state close-coupling (CC) calculation;[5] the authors present their results as a collision strength averaged over a Maxwellian electron distribution. The literature contains only one report of a measurement of electron-impact excitation for this ion.[6]

In this work we have undertaken some close-coupling calculations of the $Al^{2+}$ system at two different levels. Both five- (3*s*, 3*p*, 3*d*, 4*s*, and 4*p*) and nine-state ($+\overline{4d}$, $\overline{4f}$, $\overline{5s}$, and $\overline{5p}$) calculations have been performed. One- and two-body polarization potentials have been included at all stages of the calculations. In order to test the accuracy of the (unitarized) Coulomb-Born approximation, we also report results for this approximation using exactly the same wave functions and polarization potentials.

The remainder of this paper is arranged as follows. In Sec. II we discuss the calculation of the $Al^{2+}$ bound-state wave functions and report oscillator strengths for the various states included in the close-coupling expansion. We also discuss the different approximations used for the scattering and bound-state calculations. In Sec. III we report the results of our calculations of $Al^{+}$ bound-state energies. The results of our calculations for excitation of the 3*s*-3*p* transition are presented in Sec. IV and compared with the results of other investigations. In Sec. V we present results for excitation of the 3*d*, 4*s*, and 4*p* levels, all of which contribute by cascade to the emission cross section for the 3*p* state. Finally, we summarize our results in Sec. VI and discuss their implications.

## II. DETAILS OF THE CALCULATION

Since the $Al^{2+}$ ion can be thought of as a loosely bound valence electron outside a tightly bound neonlike core, a simple semiempirical model can be used to describe the $Al^{2+}$ ground- and excited-state wave functions. As a first approximation we can use a fixed-core Hartree-Fock model to describe the structure of the $Al^{2+}$ ion. The primary defect of such an approach is that it does not allow for the polarization of the core electrons by the charge cloud of the valence electron. The effects of core polarization are included using the semiempirical approach. Once we have constructed the fixed-core Hartree-Fock (HF) wave functions the details of the semiempirical polarization potentials can be determined by the requirement that the calculated binding energies of the $Al^{2+}$ valence states be the same as the experimental binding energies. This approach has the advantages of being computationally inexpensive as well as providing a natural extension to the second "scattered" electron.

In order to initiate our calculations we performed a series of single-configuration HF calculations of $Al^{2+}$ states using the numerical program of Froese-Fischer.[7] Koopman energies for the valence states determined from calculations using a relaxed core and fixed core (determined by calculations of the 3*s* state) are given in Table I. It is clear that the calculations using the fixed core provide a reasonable approximation to the fully relaxed HF calculations.

Analytic HF wave functions, expressed in terms of a Slater-type-orbital (STO) basis were ultimately used for the scattering calculation. The primary reason for this is

TABLE I. Theoretical and experimental binding energies (in a.u.) for the low-lying valence states of $Al^{2+}$. The experimental binding energies are averaged over the spin-orbit splitting. We use the abbreviations NHF and AHF to distinguish between single configuration HF calculations undertaken with the Froese-Fischer program (Ref. 7) and those done with the Slater-type-orbital expansion technique.

| State | NHF relaxed core | NHF fixed 3s core | AHF fixed 3s core | AHF fixed 3s core + $V_{pol}$ | Expt.[a] |
|---|---|---|---|---|---|
| 3s | −1.031 056 | −1.031 056 | −1.031 052 | −1.045 433 | −1.045 433 |
| 3p | −0.791 072 | −0.791 346 | −0.791 354 | −0.800 126 | −0.800 126 |
| 3d | −0.512 131 | −0.512 374 | −0.512 375 | −0.517 089 | −0.517 089 |
| 4s | −0.466 271 | −0.466 530 | −0.466 521 | −0.470 326 | −0.470 586 |
| 4p | −0.387 686 | −0.387 904 | −0.387 898 | −0.390 549 | −0.390 746 |

[a] Reference 8.

that the polarization potential has been included in our analytic HF program, while there is no provision for the inclusion of a polarization potential in the numerical HF program of Froese-Fischer. It is seen in Table I that the present Koopman energies calculated with the analytic HF program for a 3s fixed core are in excellent agreement with the numerical HF Koopman energies.

Having adopted the 3s core, the description of the valence states was improved by including the semiempirical polarization potential in the Hamiltonian and recomputing the wave functions for the valence states. We chose a form for the polarization potential initially adopted by Norcross and Seaton,[9]

$$V_{pol}=\frac{-\alpha_d}{2r^4}[1-\exp(-r^6/\rho_l^6)] \ . \qquad (1)$$

The value for the static dipole polarizability ($\alpha_d$) of the $Al^{3+}$ core in the above expression was taken to be $0.268a_0^3$ ($a_0$ is the Bohr radius). This value was chosen by scaling the result obtained from a perturbed HF calculation as follows. Calculations of the dipole polarizability of $Mg^{2+}$ using Hartree-Fock[10] and configuration-interaction (CI) (Refs. 11 and 12) wave functions yielded values of $0.514a_0^3$ and $0.481a_0^3$, respectively. We used the quotient of these two values (0.481/0.514) to rescale the value ($0.287a_0^3$) calculated for $Al^{3+}$ in the HF approximation.[10] The values of $\rho_l$ in expression (1) were determined by the requirement that the computed binding energies be the same as the experimental binding energies averaged for spin-orbit splitting. The values of $\rho_l$ so determined were $0.8968a_0$, $0.9872a_0$, $1.1860a_0$, and $1.09a_0$, respectively, for $l=0$, 1, 2, and 3.

The use of the polarization potential results in immediate improvement in the binding energies, which can be expected to affect the scattering calculation. The binding energies obtained with the semiempirical wave functions (fifth column of Table I) agree with the experimental binding energies to an accuracy of better than 0.1%. The HF binding energies on the other hand have an overall accuracy of about 1%. Since the same core potential was used for states with the same $l$ value, the semiempirical wave functions are orthogonal to quite a high degree of precision; any residual nonorthogonality was removed by the Schmidt orthogonalization procedure.

A further test of the quality of our wave functions lies in the calculation of the oscillator strengths between those states to be included in the close-coupling expansion. A comparison of the absorption oscillator strengths, calculated at various levels of approximation, is given in Table II. Also shown in Table II are measured oscillator strengths from a number of sources. More accurate values of the oscillator strengths require that a core-polarization correction be made to the dipole operator.[12,15] Oscillator strengths computed using a modified dipole operator,

$$\mathbf{r}'=\mathbf{r}-\frac{\alpha_d\hat{\mathbf{r}}}{r^2}[1-\exp(-r^6/\bar{\rho}^6)]^{1/2} \qquad (2)$$

are also given in Table II. The value of $\bar{\rho}$ in the above expression was taken to be $1.04a_0$. This value is just the average of $\rho_l$ for $l$ between 0 and 3. It should be mentioned that this correction is motivated by the same basic physics used to justify the use of a dielectronic polarization potential in the scattering calculation.[9]

There is good agreement between the present *ab initio* HF $f_l$ values and the relativistic HF values of Migdalek.[13] This demonstrates that relativistic modifications to the wave functions (and the dipole integral) are minor. Perhaps the most interesting feature of this table is the excellent agreement between the semiempirical oscillator strengths and the multiconfiguration HF (MCHF) values of Froese-Fischer.[14] The MCHF oscillator strengths are the most precise currently available, using a large configurational basis to include the effects of core relaxation and core polarization. The excellent agreement with the MCHF results gives us confidence in the basic correctness of the semiempirical approach. The experimental $f$ values for the resonance transition are consistently smaller than the calculated values. This is not surprising since the experimental data are derived from beam-foil measurements, which often yield systematically longer lifetimes (i.e., smaller $f$-values) due to cascade effects.[19]

Having decided to do scattering calculations with a basis supplemented by the inclusion of pseudostates, it is necessary to specify how the pseudostates were chosen. There are a number of criteria that we wish the pseudostate basis to satisfy. First, we would like to use a degen-

TABLE II. Comparison of absorption oscillator strengths of $Al^{2+}$ calculated in a number of different approximations with experiment. We present oscillator strengths computed with both *ab initio* and semiempirical HF wave functions. The semiempirical oscillator strengths include the core-polarization correction to the dipole-length matrix element.

| | *Ab initio* HF | | Semiempirical HF with modified operator | Other theory | | |
|---|---|---|---|---|---|---|
| | | | | RHF[a] | MCHF[b] | |
| Transition | $f_l$ | $f_v$ | $f_l$ | $f_l$ | $f_l$ | Expt. |
| 3*s*-3*p* | 0.879 | 0.869 | 0.833 | 0.873 | 0.834 | 0.75±0.07[c]<br>0.81±0.08[d]<br>0.77±0.03[e] |
| 3*s*-4*p* | 0.013 | 0.013 | 0.016 | 0.014 | 0.016 | |
| 3*p*-4*s* | 0.129 | 0.129 | 0.132 | 0.131 | 0.132 | 0.15±0.02[d] |
| 3*p*-3*d* | 0.927 | 0.945 | 0.891 | 0.915 | | 0.72±0.08[c]<br>0.71±0.04[e] |
| 4*s*-4*p* | 1.289 | 1.280 | 1.278 | | 1.277 | |
| 3*d*-4*p* | 0.171 | 0.176 | 0.171 | | | |

[a] Relativistic Hartree-Fock, Ref. 13.
[b] Multiconfiguration Hartree-Fock, Ref. 14.
[c] Reference 16.
[d] Reference 17.
[e] Reference 18.

erate pseudostate basis; this greatly facilitates the solution of the close-coupling equations in the asymptotic region and makes it possible to characterize the pseudostate basis by one parameter, namely the excitation energy ($\bar{\varepsilon}$) of the pseudostates above the ground state. Second, since we wish to do scattering calculations up to a maximum incident electron energy of 1.0 a.u., the pseudostate excitation threshold should be at an energy of at least 1.2 a.u. above the ground state, otherwise the presence of spurious pseudoresonances associated with the pseudostates would cause the cross sections to be of dubious accuracy near the pseudostate thresholds. Some preliminary calculations showed that neither binding energies nor partial cross sections (for 3*p* excitation) were sensitive to small changes in $\bar{\varepsilon}$ (between 1.3 and 1.5 a.u.). Since one value of $\bar{\varepsilon}$ is as good as any other, $\bar{\varepsilon}$ was fixed at 1.3 a.u.

The exact radial form adopted for the pseudostates is similar to that adopted in a previous calculation[20] for $Be^+$. The pseudostates were chosen to have the functional form

$$\bar{\Psi}_{nl}(r)=0.002\left[\frac{[2Z/(l+1)]^{2l+1}}{(2l)!}\right]^{1/2} r^{l-1} \times\exp[-Zr/(l+1)] +1.0\left[\frac{(2\alpha_{nl})^{2n+1}}{(2n)!}\right]^{1/2} r^{n-1}\exp(-\alpha_{nl}r)\ , \quad (3)$$

where $Z$ is the nuclear charge. These orbitals were Schmidt orthogonalized to the lower-lying 1*s*-4*p* orbitals. The parameters $\alpha_{nl}$ were then adjusted until the excitation energies of the pseudostates were equal to 1.3 a.u. within a certain tolerance (e.g., $< 10^{-5}$ a.u.).

We performed a number of different scattering calculations for the $Al^{2+}$ system. While these calculations often used quite different approaches, the same set of bound-state wave functions was generally used. Since the core-polarization potential was used in constructing the $Al^{2+}$ valence states, it was also included in the Hamiltonian for the second scattered electron for reasons of consistency. Note that a value of $1.09a_0$ was uniformly adopted for $\rho_l$ for $l \geq 3$. The two-body dielectronic polarization potential was also included in the Hamiltonian. The form adopted for this potential is

$$V_{\text{diel}}(r_1,r_2)=-\alpha_d\frac{\hat{\mathbf{r}}_1\cdot\hat{\mathbf{r}}_2}{r_1^2r_2^2}\{[1-\exp(-r_1^6/\rho'^6)] \times[1-\exp(-r_2^6/\rho'^6)]\}^{1/2}\ . \quad (4)$$

A value of 1.04 a.u. was adopted for $\rho'$.

The different calculations are now described in order of increasing complexity.

(i) UCBAV5. This was a fully unitarized Coulomb-Born calculation (with exchange up to a total angular momentum $L$ of 10) with on-shell coupling included between five states (3*s*, 3*p*, 3*d*, 4*s*, 4*p*). One- and two-body polarization potentials were included in the scattering calculation.

(ii) CC5. This is the only calculation in which we did *not* include polarization potentials. Five states (3*s*, 3*p*, 3*d*, 4*s*, 4*p*) were explicitly included in the close-coupling approximation. These states were represented by the fixed-core analytic HF wave functions and the polarization potentials were omitted.

(iii) CCV5. This calculation is the same as the CC5 calculation except that the semiempirical HF wave functions were used and the one- and two-body polarization potentials were included in the scattering Hamiltonian.

(iv) CCV9. This calculation is the same as the CCV5 calculation except that an additional four pseudostates ($\overline{4d}$, $\overline{4f}$, $\overline{5s}$, and $\overline{5p}$) were explicitly coupled together in the close-coupling expansion. A fine energy mesh ($\leq 0.01$ a.u.) was used to map out the resonance structure for incident energies below the $4p$ threshold.

The close-coupling calculations described above were performed using the COLALG (Ref. 21) and IMPACT (Ref. 22) suite of programs. The program IMPACT was used to solve the CC equations up to a maximum $L$ value of 12. We included exchange terms with a maximum polarity of up to 10 in the kernel of the integrodifferential equations. The higher partial waves were taken into account using the five-state unitarized Coulomb-Born approximation (UCBAV5). The close-coupling calculations using the polarization potentials (i.e., CCV5 and CCV9) used UCBAV5 reactance matrices to complete the partial-wave sum. Unitarized Coulomb-Born reactance matrices computed without any polarization potentials and using *ab initio* HF wave functions were used to complete the partial-wave sum for the CC5 calculation. The error introduced into the excitation cross sections by switching from close-coupling to Coulomb-Born reactance matrices at $L=13$ was less than 1% at all the energies considered in this paper.

## III. BINDING ENERGIES OF $\mathrm{Al}^+$

The binding energies of the $\mathrm{Al}^+$ system provide a supplementary test of the accuracy of our model of the $e^-$-$\mathrm{Al}^{2+}$ system as well as being intrinsically interesting. A previous binding energy calculation on the Be atom[20] using the same semiempirical approach as the present work gave binding energies which are in excellent agreement with experiment. The present calculations confirm that this method can be extended to larger atoms and still be expected to give reliable binding energies.

A tabulation of binding energies for a number of states of the $\mathrm{Al}^+$ ion, computed using a number of different approaches, is given in Table III. Comparison of the HF and CI calculations of Weiss[23,24] demonstrates conclusively that CI effects are quite important. The calculation of Weiss allowed for CI effects within the two valence electrons, but the ten core electrons were fixed. Since the basic physics of this calculation is essentially identical to the purely *ab initio* CC5 calculation, it is not surprising that the CC5 binding energies are generally consistent with the CI results.

The inclusion of the polarization potentials in the CC5V and CC9V calculations markedly changes the binding energies. The polarization potential usually causes an increase in the binding energy, leading to significantly better agreement with experiment. A good example of the importance of this effect occurs for the $3s3p\ ^1P^o$ level. Comparison of the CC5 and CC5V levels reveals that inclusion of the polarization potential causes a increase in the binding energy of 0.005 12 a.u. Since the difference between the CC5 and experimental binding energies is only 0.006 86 a.u., the polarization potential plays a large part in reducing the discrepancy between theory and experiment.

Another of the interesting consequences of the polarization potential occurs for those states (the $3p^2\ ^1D^e$, $3s4f\ ^1F^o$, and $^3F^o$ states) for which the CI and CC5 calculations predict larger binding energies than experiment. This implies a breakdown of the variational theorem unless interactions between the valence and core electrons (e.g., core polarization) can lead to a decrease in the binding energy. In all these cases, inclusion of the core-

TABLE III. Binding energies (in a.u.) of a number of low-lying $\mathrm{Al}^+$ bound states relative to the $\mathrm{Al}^{2+}$ $3s$ series limit. The experimental binding energies of the triplet states correspond to the center of gravity of the different $J$ states.

| State | HF[a] | CI[a] | CC5 | CC5V | CC9V | Expt.[b] |
|---|---|---|---|---|---|---|
| $3s^2\ ^1S^e$ | 0.6437 | 0.6839 | 0.683 25 | 0.689 60 | 0.690 40 | 0.691 93 |
| $3s4s\ ^1S^e$ | 0.2438 | 0.2558 | 0.255 66 | 0.256 40 | 0.256 72 | 0.257 49 |
| $3p^2\ ^1S^e$ | 0.1582 | 0.1811 | 0.177 98 | 0.177 70 | 0.180 89 | 0.183 27 |
| $3s4s\ ^3S^e$ | 0.2674 | 0.2741 | 0.274 16 | 0.275 77 | 0.275 82 | 0.276 06 |
| $3s3p\ ^1P^o$ | 0.3730 | 0.4130 | 0.412 34 | 0.417 46 | 0.418 24 | 0.419 20 |
| $3s4p\ ^1P^o$ | | | 0.203 31 | 0.204 25 | 0.204 50 | 0.204 77 |
| $3s3p\ ^3P^o$ | 0.5122 | 0.5193 | 0.518 90 | 0.519 65 | 0.519 90 | 0.521 42 |
| $3s4p\ ^3P^o$ | | | 0.210 65 | 0.211 02 | 0.211 07 | 0.211 54 |
| $3p^2\ ^3P^e$ | 0.2539 | 0.2635 | 0.262 75 | 0.261 86 | 0.262 38 | 0.263 11 |
| $3p^2\ ^1D^e$ | 0.2149 | 0.3044 | 0.304 56 | 0.301 54 | 0.301 69 | 0.302 45 |
| $3s3d\ ^1D^e$ | 0.2217 | 0.1881 | 0.188 49 | 0.189 48 | 0.190 01 | 0.190 32 |
| $3s4d\ ^1D^e$ | | | 0.122 04 | 0.122 71 | 0.123 12 | 0.123 33 |
| $3s3d\ ^3D^e$ | 0.2472 | 0.2551 | 0.255 33 | 0.256 28 | 0.256 44 | 0.256 57 |
| $3s4d\ ^3D^e$ | | | 0.137 81 | 0.138 29 | 0.138 40 | 0.138 42 |
| $3s4f\ ^1F^o$ | | | 0.129 65 | 0.129 33 | | 0.129 36 |
| $3s4f\ ^3F^o$ | | 0.1281 | 0.130 02 | 0.129 54 | | 0.129 59 |

[a] Hartree-Fock and configuration-interaction binding energies taken from Refs. 23 and 24.
[b] Reference 8.

polarization potential results in a decrease in the binding energies, and the CC5V and CC9V binding energies are now smaller than experiment.

## IV. EXCITATION OF THE RESONANCE TRANSITION

Total cross sections for the $Al^{2+}$, $3s$-$3p$ transition are given in Table IV for a large variety of theoretical approaches. We have taken the liberty of interpolating previously published[4] cross section data for presentation in Table IV. One feature is apparent from a comparison of the CC5 and CCV5 calculations: the use of polarization potentials and semiempirical wave functions results in a substantially lower total excitation cross section. The same effect was even more pronounced in a previous calculation[25] of the electron-impact excitation of $Ca^+$.

The two perturbation theory results, namely, the UCBAV5 and the distorted-wave cross sections, have relatively large differences ( $\geq 20\%$) at all energies. Since we have few details about the distorted-wave calculation or the target wave functions employed, we can only speculate as to the reasons for the differences. Certainly contributing to the difference is core polarization, which (compare the CC5 and CCV5 results) is roughly a 10% effect.

Comparison of the UCBAV5 cross section with the CCV5 and CCV9 results reveals that this conceptually simple approximation does a surprisingly good job of reproducing the results of the close-coupling calculations. At the highest energy considered, the UCBAV5 and CCV5 cross sections differ by less than 5%. Even at the lowest energy, just above the $3p$ threshold, the UCBAV5 cross sections exceed the CCV5 results by less than 15%. However, it would be dangerous to generalize this result. A detailed comparison of UCBAV5 and CCV5 partial cross sections at the lowest energies shows that there is a fortuitous cancellation of the differences between the two calculations. The UCBAV5 predicts smaller partial cross sections at small $L$ values, and larger partial cross sections for larger $L$ values. A similar effect was noticed in the previous study[25] of $Ca^+$.

The other significant feature of Table IV is the good agreement between the CCV5 and CCV9 cross sections. At all the energies considered, the CCV5 and CCV9 cross sections agree to within 2%. This would indicate that the cross section for excitation of the $3p$ level, at least, has more or less converged with respect to increasing the number of target states included in the CC expansion.

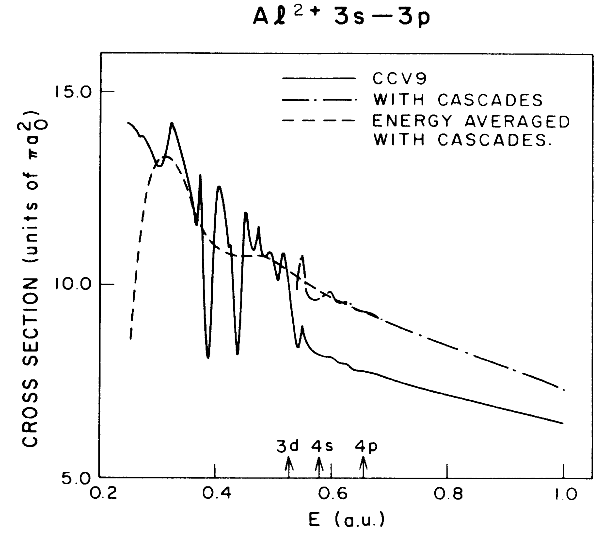

FIG. 1. Absolute emission cross section (units of $\pi a_0^2$) for electron-impact excitation of the $Al^{2+}$ $3p$ level as a function of incident energy. The results of the CCV9 calculation are depicted without cascade corrections, with cascade corrections, and energy-averaged with cascade corrections.

The $3s$-$3p$ excitation cross section is shown in finer detail in Fig. 1. The CCV9 calculation predicts two relatively wide and deep minima in the cross section at incident energies of about 0.39 and 0.44 a.u. The finite energy resolution typical of crossed electron-ion beam measurements such as that reported by Belic *et al.*[6] will to some extent obscure the resonance structure apparent in Fig. 1, and will soften the formally finite onset of the cross section at threshold. A measured *emission* cross section also includes indirect contributions to the radiation emitted by the $3p$ excited state due to cascading from higher states also excited by the electron beam. All three of these effects are illustrated in Fig. 1, where the contribution to the emission cross section from cascades from the $3d$, $4s$, and $4p$ states (discussed in more detail below) is included, and the cross section is averaged over a hypothetical Gaussian electron beam energy profile with a width of 1.5 eV. The maximum in the resulting effective cross section then becomes $11.7 \times 10^{-16}$ cm$^2$, and occurs at about 1.7 eV above the excitation threshold of 6.67 eV.

TABLE IV. Comparison of excitation cross sections (units of $\pi a_0^2$) for the $3s$-$3p$ transition in $Al^{2+}$ computed in a variety of approaches.

| | Energy (a.u.) | | | | | | |
|---|---|---|---|---|---|---|---|
| | 0.25 | 0.30 | 0.40 | 0.50 | 0.60 | 0.80 | 1.00 |
| UDW[a] | 19.7 | 17.5 | 14.5 | 12.7 | 11.3 | 9.5 | 8.3 |
| UCBAV5 | 16.30 | 14.60 | 12.32 | 10.81 | 8.90 | 7.57 | 6.73 |
| CC5 | 15.93 | 13.57 | 13.56 | 11.72 | 9.00 | 7.84 | 7.12 |
| CCV5 | 14.24 | 13.06 | 11.76 | 10.91 | 8.12 | 7.14 | 6.48 |
| CCV9 | 14.17 | 13.07 | 11.65 | 10.70 | 8.13 | 7.14 | 6.41 |

[a] Unitarized distorted wave, Ref. 4.

This is almost 25% smaller than the preliminary result for the near-threshold cross section ($16\pm3\times10^{-16}$ cm$^2$) reported by Belic *et al.*[6]

We relate the collision strength

$$\Omega_{ij}=(2L_i+1)(2S_i+1)k_i^2Q_{ij} \tag{5}$$

to the cross section $Q_{ij}$ for excitation of level $j$ from level $i$, and $k_i$ is the incident electron momentum. For $Q_{ij}$ in units of $\pi a_0^2$, and $k$ in atomic units ($a_0^{-1}$), $\Omega_{ij}$ is dimensionless. The behavior of the collision strength for excitation of the 3*p* state is shown in Fig. 2. The cascade correction, as estimated from the UCBAV5 results, is seen to be relatively constant.

In order to compare our results with the five-state close-coupling calculation of Dufton and Kingston[5] we have converted our CCV9 cross sections to collision strengths and averaged them with a Maxwellian energy distribution. We were unable to carry out this kind of analysis with our CC5 and CCV5 results owing to the coarser energy mesh used for these calculations in the resonance region. At high temperatures, it was necessary to extrapolate our calculated cross sections to energies higher than the 1.0-a.u. upper limit for the CCV9 calculations. This was done by assuming that the cross sections could be modelled by their asymptotic form. The collision strengths for the 3*s*-3*d* and 3*s*-4*s* transitions were assumed to be constant at energies larger than 1.0 a.u. This assumption was supported by UCBAV5 calculations carried out for energies up to 5.0 a.u. The dipole-allowed transitions were modelled by a collision strength that increased logarithmically, as illustrated by Fig. 2. Although the extrapolation procedure will introduce errors into the effective collision strengths at high temperatures, the errors are not so large as to prevent a meaningful comparison with the results of Dufton and Kingston. We estimate the error in the 3*p* collision strength to be less than 5% and the error in the 4*p* collision strength to be less than 20%. At the lowest temperatures reported in Table V the errors due to extrapolation are much smaller.

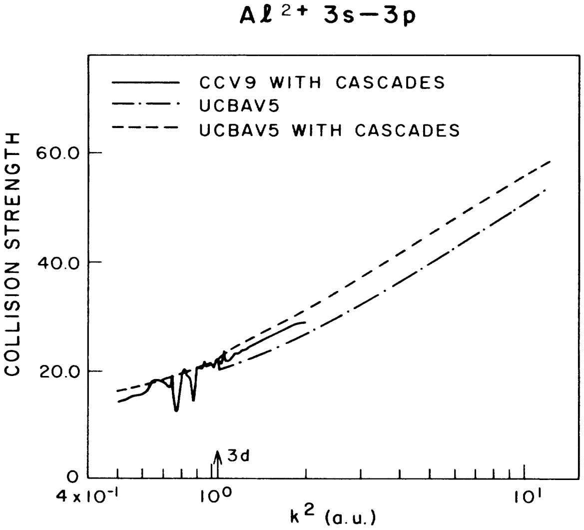

FIG. 2. Collision strength for the resonant 3*s*-3*p* excitation of Al$^{2+}$ as a function of the square incident electron momentum, $k^2$. The results of the UCBAV5 calculation, with and without cascade corrections, are depicted. The results of the CCV9 calculation (with cascade correction) are also shown.

TABLE V. Effective collision strengths for excitation of the four lowest levels of Al$^{2+}$. In all cases collision strengths derived from the present CCV9 calculation are given above those of Ref. 5.

| | $\log_{10}T_e$ | | | | |
|---|---|---|---|---|---|
| Transition | 4.0 | 4.3 | 4.6 | 4.9 | 5.2 |
| 3*s*-3*p* | 15.2 | 16.0 | 17.2 | 18.9 | 21.3 |
| | 16.0 | 17.3 | 19.1 | 21.5 | 24.9 |
| 3*s*-3*d* | 2.60 | 2.80 | 2.90 | 2.92 | 2.88 |
| | 3.90 | 3.84 | 3.86 | 3.98 | 4.12 |
| 3*s*-4*s* | 0.84 | 0.86 | 0.83 | 0.77 | 0.70 |
| | 1.17 | 1.13 | 1.10 | 1.09 | 1.11 |
| 3*s*-4*p* | 0.43 | 0.42 | 0.39 | 0.35 | 0.32 |
| | 0.61 | 0.61 | 0.62 | 0.63 | 0.62 |

A comparison of effective collision strengths from the present calculation and those of Dufton and Kingston is given in Table V. The present effective CCV9 collision strength for 3*p* excitation is some 5–10% smaller in magnitude at all temperatures than that of Dufton and Kingston. Since the calculation of Dufton and Kingston couples the same levels as the present CC5 calculation, and the effect of resonances is included in both calculations, we would expect it to give qualitatively similar results. The differences evident in Table V for the 3*p* cross section are therefore consistent with the differences of about 10% reported between the present CC5 and CCV9 calculations (see Table IV).

## V. EXCITATION OF THE 3*d*, 4*s*, AND 4*p* LEVELS

In this section we report cross sections for excitation of the 3*d*, 4*s*, and 4*p* states levels from the ground state. The results are shown in Fig. 3, and a comparison of cross sections obtained in the different approaches is given in Table VI. The scatter among the results from different calculations is larger than it was for the resonant 3*s*-3*p* excitation. This is not unexpected; the relatively larger excitation energies and the nondipole nature of the 3*d* and 4*s* transitions will result in excitations that are not dominated to the same extent by long-range interactions (i.e., high partial waves) as is the resonance transition. The 4*p* excitation is a dipole transition, but consideration of the oscillator strength given in Table II suggests that the long-range nature of the collision process is unlikely to be dominant. Hence a larger contribution to the cross section will come from the low partial waves where both distortion and coupling effects are quite substantial.

The comparison of the CCV5 and UCBAV5 cross sections reveals the inadequacy of perturbation theory for these transitions. At threshold the differences between the UCBAV5 and CC5 calculations are never less than 25% and can be as large as a factor of 2. The differences

TABLE VI. Total excitation cross sections (units of $\pi a_0^2$) at some representative energy points for electron-impact excitation of the $Al^{2+}$ $3d$, $4s$, and $4p$ levels from the ground state.

| | Energy (a.u.) | | | | | |
|---|---|---|---|---|---|---|
| | 0.55 | 0.6 | 0.7 | 0.8 | 0.9 | 1.0 |
| | | | | $3d$ | | |
| UCBAV5 | 1.18 | 1.15 | 1.07 | 0.992 | 0.992 | 0.860 |
| CCV | 1.56 | 1.50 | 1.42 | 1.19 | 1.10 | 1.01 |
| CCV5 | 1.95 | 1.35 | 1.20 | 1.11 | 1.02 | 0.941 |
| CCV9 | 1.84 | 1.23 | 1.08 | 0.961 | 0.828 | 0.691 |
| | | | | $4s$ | | |
| UCBAV5 | | 0.246 | 0.226 | 0.203 | 0.185 | 0.171 |
| CC5 | | 0.675 | 0.357 | 0.327 | 0.299 | 0.275 |
| CCV5 | | 0.473 | 0.354 | 0.324 | 0.298 | 0.275 |
| CCV9 | | 0.420 | 0.291 | 0.254 | 0.209 | 0.135 |
| | | | | $4p$ | | |
| UDW[a] | | | 0.199 | 0.162 | 0.136 | 0.118 |
| UCBAV5 | | | 0.140 | 0.115 | 0.095 | 0.081 |
| CC5 | | | 0.251 | 0.192 | 0.171 | 0.153 |
| CCV5 | | | 0.194 | 0.173 | 0.153 | 0.135 |
| CCV9 | | | 0.154 | 0.122 | 0.089 | 0.056 |

[a] Unitarized distorted wave, Ref. 4.

are not much smaller at the highest energy (1.0 a.u.) considered, but the incident energy is still less than twice the excitation energy of all of these levels. There are also significant differences between the CCV5 and CCV9 cross sections. The CCV9 cross sections are smaller in magnitude than the CC5 and CCV5 results at all energies and for all transitions. This difference is reflected in the effective (Maxwellian-averaged) collision strengths given in Table V, where the CCV9 results are compared to those of Dufton and Kingston.[5] The latter were obtained using cross sections from a calculation much closer in spirit to our CC5 calculation.

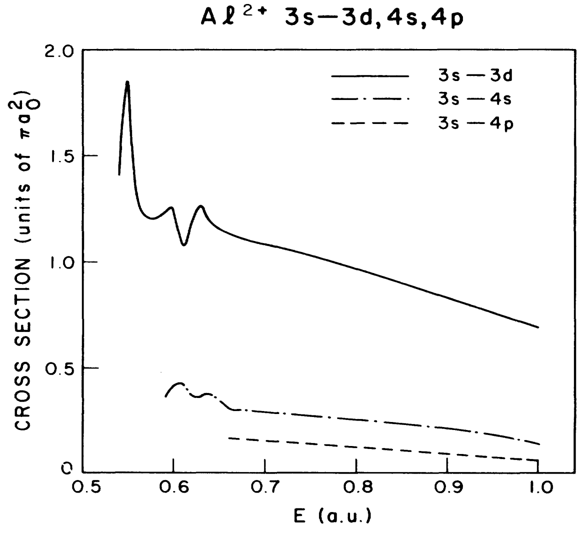

FIG. 3. Total cross sections (units of $\pi a_0^2$) for excitation of the $Al^{2+}$ $3d$, $4s$, and $4p$ levels from the ground state as a function of the incident energy (in a.u.). The results of the CCV9 calculation are depicted.

Since essentially all experimentally derived cross sections for electron-ion excitation have resulted from emission measurements,[26] we have also computed, and displayed in Fig. 1, an illustrative emission cross section for the $3p$ excitation. The emission cross section for the $3p$ state will be sensitive to cascades from excitations to the $3d$, $4s$, and $4p$ levels. While excitations of the $3d$ and $4s$ levels always result in decay (in the dipole approximation) to the $3p$ state, this is not true for excitations of the $4p$ level. The $4p$ state must first decay into either the $3d$ or $4s$ states, which then feeds into the $3p$ state. The $4p$ state can also decay directly into the $3s$ ground state. We have determined the branching ratio for the $4p$ state to cascade into the $3p$ level by converting the oscillator strengths given in Table II into transition rates. We find that excitation of the $4p$ level will eventually decay into the $3p$ state 61% of the time. Using this number we derive the following expression for the effective emission cross section ($Q_{em}$) of the $3p$ state:

$$Q_{em} = Q_{3p} + Q_{3d} + Q_{4s} + 0.61 Q_{4p} . \tag{6}$$

The cascade corrections to the $3p$ emission cross section and collision strength are depicted in Figs. 1 and 2, respectively. At energies just above the $4p$ excitation threshold, the increase in the emission cross section due to cascades is about 20%. At the highest energy for which close-coupling cross sections were obtained, the cascade correction is about 12%. The behavior of the cascade correction at much higher energies is shown in Fig. 2. At the highest value of $k^2$ (corresponding to an incident energy of 6.0 a.u.) for which the UCBAV5 calculations were performed the cascade correction is less than 10%. At still higher energies the cascade correction becomes smaller, dropping to about 5% at 15 a.u. according to the unitarized distorted-wave (UDW) results.[4]

## VI. CONCLUSIONS

We have performed a series of close-coupling and unitarized Coulomb-Born calculations for electron-impact excitation of the valence electron in $Al^{2+}$. Inclusion of the core-polarization potentials leads to a reduction of almost 10% in the excitation cross section for the resonance transition. This result, considered in conjunction with a similar effect[25] for potassiumlike $Ca^+$, is an indication that the polarization potentials are an important part of the Hamiltonian for the heavier alkali-metal-like ions (the effect was shown[20] to be much smaller for lithiumlike $Be^+$). Further confirmation of the importance of polarization potentials is illustrated by the calculations reported here for the $Al^+$ binding energies. In every case, inclusion of the polarization potentials results in improved agreement with experimental binding energies. Comparison of the CC5V (five states) and CC9V (five states plus four pseudostates) cross sections for the resonance transition indicates that the cross section for this transition has converged at least with respect to increasing numbers of channels. This is not true for excitation of higher levels (the 3*d*, 4*s*, and 4*p* states), where there are large differences between the CC5V and CC9V cross sections.

## ACKNOWLEDGMENTS

This work has been partially supported by the United State Department of Energy (Division of Chemical Sciences, Office of Basic Energy Sciences, Office of Energy Research). The calculations performed in this work were done with the Control Data Corporation Cyber 205 at National Bureau of Standards (NBS) Gaithersburg, and the Digital Electronics Corporation VAX 8600 at the Joint Institute for Laboratory Astrophysics.

---

[*] Present address: Department of Theoretical Physics, Research School of Physical Sciences, The Australian National University, G.P.O. Box 4, Canberra, Australian Capital Territory 2601, Australia.

[†] Also at Quantum Physics Division, National Bureau of Standards.

[1] K. C. Mathur, A. N. Tripathi, and S. K. Joshi, Int. J. Mass. Spectrom. Ion Phys. **7**, 167 (1971).

[2] Y. K. Kim and K. T. Cheng, Phys. Rev. A **18**, 36 (1978).

[3] J. Davis and S. Morin, J. Quant. Spectrosc. Radiat. Transfer **11**, 495 (1971).

[4] A. L. Merts, J. B. Mann, W. D. Robb, and N. H. Magee, Jr., Los Alamos Informal Report LA-8267-MS, 1980 (unpublished); (personal communication).

[5] P. L. Dufton and A. E. Kingston, J. Phys. B **20**, 3899 (1987).

[6] D. S. Belic, R. A. Falk, G. H. Dunn, D. Gregory, C. Cisneros, and D. Crandall, Bull. Am. Phys. Soc. **26**, 1315 (1981).

[7] C. Froese-Fischer, Comput. Phys. Commun. **14**, 145 (1978).

[8] S. Bashkin and J. O. Stoner, *Atomic Energy Levels and Grotrian Diagrams* (North-Holland, Amsterdam, 1975), Vol. 3.

[9] D. W. Norcross and M. J. Seaton, J. Phys. B **9**, 2983 (1976).

[10] S. Fraga and J. Muszynska, *Atoms in External Fields* (Elsevier, Amsterdam, 1981).

[11] H.-J. Werner and W. Meyer, Phys. Rev. A **14**, 915 (1976).

[12] W. Muller, J. Flesch, and W. Meyer, J. Chem. Phys. **80**, 3297 (1984).

[13] J. Migdalek, Can. J. Phys. **54**, 130 (1976).

[14] C. Froese-Fischer, Can. J. Phys. **54**, 1465 (1976).

[15] S. Hameed, A. Herzenberg, and M. G. James, J. Phys. B **1**, 822 (1968); S. Hameed, *ibid.* **5**, 746 (1972).

[16] H. G. Berry, J. Bromander, and R. Buchta, Phys. Scr. **1**, 181 (1970).

[17] Y. Baudinet-Robinet, P. D. Dumont, H. P. Garnir, E. Biemont, and N. Grevesse, J. Phys. (Paris) Colloq. C1 Suppl. 2, **40**, 175 (1976).

[18] J. A. Kernahan, E. H. Pinnington, J. A. O'Niell, R. L. Brooks, and K. E. Donnelly, Phys. Scr. **19**, 267 (1979).

[19] R. J. S. Crossley, L. J. Curtis, and C. Froese-Fischer, Phys. Lett. **57**, 220 (1976).

[20] J. Mitroy and D. W. Norcross, Phys. Rev. A **37**, 3755 (1988).

[21] This program is unpublished. Recent references are P. G. Burke and W. Eissner, in *Atoms in Astrophysics*, edited by P. G. Burke, W. Eissner, D. G. Hummer, and I. C. Percival (Plenum, New York, 1983), p. 1; and H. Nussbaumer and P. J. Storey, in *ibid.*, p. 265.

[22] M. A. Crees, M. J. Seaton, and P. M. H. Wilson, Comput. Phys. Commun. **15**, 23 (1978).

[23] A. Weiss, J. Chem. Phys. **47**, 3573 (1967).

[24] A. Weiss, Phys. Rev. A **9**, 1524 (1974).

[25] J. Mitroy, D. C. Griffin, D. W. Norcross, and M. S. Pindzola, Phys. Rev. A **38**, 3339 (1988).

[26] K. Dolder and B. Peart, Adv. At. Mol. Phys. **22**, 197 (1986).